Multi-target trust region parameter-guided optimization algorithm and its application in design of film-covered sweet potato transplanting mechanism

Xingxiao Ma[1], Xiong Zhao[1,2*], Jianneng Chen[1,2], Gaohong Yu[1,2], Bingliang Ye[1]

(1. *Faculty of Mechanical Engineering and Automation, Zhejiang Sci-Tech University, Hangzhou 310018, China*;
2. *Key Laboratory of Crop Harvesting Equipment Technology of Zhejiang Province, Jinhua 321017, Zhejiang, China*)

Abstract: The film-covered sweet potato transplanting method requires ensuring the transplantation conditions of small planting holes and large lateral displacement. In the soil insertion phase, the transplantation machine requires a mechanism design with multiple timed poses, and the existing design methods are still imperfect. For this reason, this article proposes a multi-target trust region parameter-guided optimization algorithm. This algorithm aims to achieve multi-objective optimization design with more timed pose conditions starting from individual timed pose conditions. First, multi-target problems are decomposed into multiple subproblems, and the parameter arrays are kept with the minimum polymerization value of each subproblem. Then, the approximate function value reduction for each target is calculated using this parameter set, and the step size for the next iteration of each subproblem is determined by comparing this approximate reduction with the actual reduction. After many iteration calculations, the parameter arrays end the calculation when the parameter group is no longer updated. This paper uses the design of a film-covered sweet potato transplanting mechanism as a complex optimized application example. The algorithm is used to obtain the optimization results of the target values of eight groups of institutions. The smallest hole is 2.99 mm, and the horizontal transplanting distance is 108.40 mm. The maximum hole is 17.64 mm, and the horizontal transplanting distance is 124.97 mm. Considering the size of the hole and the horizontal transplanting distance of sweet potato transplanting, the mechanism's target value of the horizontal transplanting distance at 119.92 mm and the hole size at 0.31 mm were selected to design the sweet potato transplanting machine. The correctness of the results is verified, which reflects the practicability of the algorithm.

Keywords: optimization algorithm, multi-objective, trust region method, parameter-guided optimization algorithm, sweet potato transplanting mechanism, trajectory optimization

DOI: 10.25165/j.ijabe.20251803.9595

Citation: Ma X X, Zhao X, Chen J N, Yu G H, Ye B L. Multi-target trust region parameter-guided optimization algorithm and its application in design of film-covered sweet potato transplanting mechanism. Int J Agric & Biol Eng, 2025; 18(3): 154–164.

1 Introduction

As a crucial economic crop, sweet potatoes require automation and large-scale transplantation due to economic development and increasing labor costs[1]. Transplantation methods include direct, slanted, horizontal, and bottom insertion[2]. Soil mulching on ridges maintains soil moisture and temperature, enhancing sweet potatoes' growth[3]. Film-covered bottom planting demands precise soil insertion trajectory and minimal seedling claw damage to the film.

Current sweet-potato transplantation methods include chain-clamping, basket-type, and linkage mechanisms. Hu et al.[4] designed a 2ZGF-2 chain-clamping sweet potato transplanting machine. Li et al.[5] designed a chain-clamping sweet potato transplanting machine. Yan et al.[6] designed a sweet potato horizontal planting machine with furrow creation and spiral soil covering. These machines face challenges with accuracy over time.

In the linkage mechanisms, Pan et al.[7] designed a sweet potato transplantation machine with a four-bar linkage structure. Wen et al.[8] designed a sweet potato transplanting machine with a double-crank five-bar linkage mechanism. Liu et al.[9] and Zheng et al.[10] designed RP-type and RR-type linkage manipulators to achieve the required trajectories for sweet potato transplantation, respectively. Four-bar and two-open-chain linkage transplanting mechanisms, among others, can meet the requirements for uncovered sweet potato transplantation in terms of motion trajectories but struggle to fulfill the demands of film-covered sweet potato transplantation, where minimal film damage is crucial.

The design methods for linkage mechanisms include graphical methods [11], closed-loop vector methods[12], Fourier series methods, kinematic mapping[13], and optimization techniques. In the synthesis of single-degree-of-freedom linkage mechanisms, the crank angle information of the linkage can be used as a timing reference. Li et al.[14] conducted timed trajectory synthesis for four-bar linkages, and Yim et al.[11] employed a combination of Fourier series and deep learning for the synthesis of six-bar linkages. Fourier series method is not compatible with the requirements of controlling multiple poses during the soil insertion phase of sweet potato transplantation. Two-open-chain and four-bar linkages can achieve mechanism

Received date: 2024-12-11 **Accepted date:** 2025-04-08

Biographies: **Xingxiao Ma**, PhD candidate, research interest: agricultural machinery, Email: 2416771239@qq.com; **Jianneng Chen**, PhD, Professor, research interest: machine design, non-circular gear transmissions and agricultural machinery, Email: jiannengchen@zstu.edu.cn; **Gaohong Yu**, PhD, Professor, research interest: machine design, non-circular gear transmissions and agricultural machinery, Email: yugh@zstu.edu.cn; **Bingliang Ye**, PhD, Professor, research interest: agricultural machinery, Email: blye@zstu.edu.cn.

***Corresponding author: Xiong Zhao**, PhD, Professor, research interest: machine design, non-circular gear transmissions and agricultural machinery. Faculty of Mechanical Engineering and Automation, Zhejiang Sci-Tech University, Hangzhou 310018, China. Email: zhaoxiong@zstu.edu.cn.

synthesis with a maximum of five poses[15]. Bulatović et al.[16] accomplished timed trajectory synthesis for four-bar linkages. Baskar et al.[17] derived equations for six-bar linkages with timing constraints. It is evident that kinematic synthesis with timing constraints imposes greater demands on mechanisms.

Deng et al.[18] used a single-row planetary mechanism combined with non-circular gears. The two-open-chain linkage mechanism cannot accommodate a mechanism design method involving multiple timing sequences and pose matching. Liao et al.[19] and Hu et al.[20] proposed double planetary mechanisms with limited poses with timing informations.

Because there is a correspondence between the input timed poses and the number of equations, it is not possible to directly input an infinite amount of timed pose information during the design parameter stage. Optimization methods can achieve mechanism designs that satisfy as many specified requirements as possible. Goulet et al.[21] used Couenne's solution to obtain a four-bar mechanism that can pass more position points. Zhang et al.[22] designed a six-bar finger grasping mechanism with flexible parts by using GA. Xu et al.[23] and Zheng et al.[24] also used parameter-guided optimization algorithm to design a double-arm rice transplanting mechanism and flower seedling transplanting machines, separately. This method's disadvantage is that the step size of each solution is the same, which affects the computational efficiency or accuracy. The Pareto optimal solution set of the multi-objective problem is not obtained. Sweet potato transplantation involves two objectives: a large lateral displacement and small planting holes.

Yi et al.[25] proposed NSGA-III. Zhang et al.[26] invented the MOEAD algorithm in 2007. Wang et al.[27] used MOEAD to optimize the design of automobile collision boxes in 2022. Existing multi-objective optimization algorithms require specifying the boundaries for each parameter. Currently, research on algorithms to address such problems is relatively limited.

In this paper, a trust region parameter-guided optimization algorithm that can realize variable-step processing is designed. Based on this algorithm, combined with MOEAD's idea of transforming multi-objective problems into multiple sub-targets, a multi-target trust region parameter-guided optimization algorithm is proposed. This algorithm starts from individual timed pose conditions to implement a multi-objective optimization algorithm for sweet potato transplanting machines with more timed pose conditions. The algorithm proposed in this paper has the advantages of stable calculation results and clear iterative jump determination conditions when dealing. Finally, the optimized design of the film-covered sweet potato transplanting mechanism with transplanting trajectory requirements proves the practicability of the algorithm.

2 Trust region parameter guidance algorithm

For a single objective function $f(x)$ with u variables, the parameter guidance algorithm is to give a small step size. At the k-th iteration, after increasing or decreasing the small step size of each variable in the parameter group, a parameter $x_{i1}^{k+1}=x_i^k+\Delta x$ that increases a small amount and a parameter $x_{i2}^{k+1}=x_i^k-\Delta x$ that reduces a small amount are obtained. The variables of the previous iterative calculation are replaced, and the corresponding function values are calculated. The parameter group X_{k+1} corresponding to the minimum objective function value after the k-th iteration is taken as the parameter group of the next iteration. The method uses the same step size in each iteration, and the calculation speed and calculation accuracy cannot be combined. This section proposes a trust region parameter method to solve this problem.

At point X_k, the rate of descent $\Delta h(k)$ is desirable, but it is impossible to obtain by solving the minimum problem $\min f(X_{k+1}-X_k)$ because this problem is as difficult as directly solving the optimal value of the function $f(x)$. Therefore, this section considers the use of the trust region method to adjust the step size $\Delta h(k)$ at each iteration, which can speed up the calculation and improve the calculation accuracy.

In the k-th iteration, the step size $\Delta h(k)$ is used to calculate the optimal parameter group X_{k+1} by the parameter guidance method, and the corresponding function value $f(X_{k+1})$ is obtained. Considering the step size to be small, the gradient of the objective function at this parameter group X_k can be approximately expressed as:

$$g_k(X_k)=\nabla f(X_k)\approx\left[\frac{y_{11}^{k+1}-y_{12}^{k+1}}{\Delta h(k)},\frac{y_{21}^{k+1}-y_{22}^{k+1}}{\Delta h(k)},\ldots,\frac{y_{u1}^{k+1}-y_{u2}^{k+1}}{\Delta h(k)}\right]^{\mathrm{T}} \tag{1}$$

The first-order Taylor expansion of the objective function at this point is:

$$q_k(\Delta h_k)=f(X_k)+g_k^{\mathrm{T}}\cdot(X_{k+1}-X_k) \tag{2}$$

This Taylor expansion is used as an approximation of the function value $f(X_{k+1})$ obtained in the next step. The error between $q_k(\Delta h_k)$ and $f(X_{k+1})$ is $o(\|\Delta h_k\|^2)$. Relatively speaking, when $\|\Delta h_k\|$ is small, the error between $q_k(\Delta h_k)$ and $f(X_{k+1})$ is small. It can ensure that $q_k(\Delta h_k)$ is an approximate function of $f(X_{k+1})$. Therefore, using the degree of similarity with these $q_k(\Delta h_k)$ and $f(X_{k+1})$, a suitable field is selected at each iteration, and the step size at the next iteration is controlled to achieve variable step size parameter guidance that can increase the calculation speed and accuracy.

In the k-th iteration, the actual reduction of function $f(X)$ is $\Delta f_k=f(X_{k+1})-f(X_k)$, the reduction of the approximate function $q_k(\Delta h)$ is $\Delta q_k(\Delta h_k)=g_k^{\mathrm{T}}\cdot(X_{k+1}-X_k)$, and the ratio of the two reductions is:

$$r_k=\frac{\Delta f_k}{\Delta q_k}=\frac{f(X_{k+1})-f(X_k)}{g_k^{\mathrm{T}}\cdot(X_{k+1}-X_k)} \tag{3}$$

The ratio r_k is used to define the approximation degree of the approximate function and the original function. When the step size is small, the value is closer to 1; when the approximation is better, the step size should be increased in the next iteration. In the calculation process, when the step size is too large, it may occur that one parameter in the parameter group exceeds the corresponding parameter in the optimal parameter group during the change process. Therefore, it is necessary to ensure that the preferred parameter group is the same as the change direction in the parameter in the previous parameter group before adding the step size used in the next iteration calculation. If the value is close to a positive number of 0, indicating that the approximation is not good, the next iteration should reduce the step size. If the value is equal to 0 or negative, the selected step size is problematic, the optimal value point of the function has been missed, the trust region needs to be further reduced, and the direction of the function needs to be searched in reverse. Considering that the parameter guidance method searches the positive and negative directions of each parameter in the iterative calculation, a smaller step size should be used in the next iterative calculation, and the positive and negative values of the variable step size are not needed.

Compared with the original parameter-guided optimization algorithm, this method can define the minimum step size $\min bc$ in

the iterative calculation, that is, the final calculated variable accuracy. When the step size is large, the calculation of the approximate function $q_k(\Delta h_k)$ will produce deviation. Therefore, the maximum step size $\max bc$ should be defined. The calculation result deviating too much from the expectation or entering other local optimums due to the excessive step length in the iteration process can be avoided.

In addition, when the k-th iteration is calculated, the variable changed at that iteration is inconsistent with the previous change of the variable. The maximum step size $\max bc2$ is limited to 3/4 of the step size used in the current iteration. The maximum step size $\max bc2$ will only be updated when a parameter exceeds the optimal parameter in parameter optimization. This step can also ensure that the step size is gradually reduced when the algorithm is close to the optimal value of the function, and the algorithm converges.

The value of Δh_{k+1} is defined as follows:

$$\Delta h_{k+1} = \begin{cases} 2\Delta h_k, & r_k > 0.75 \\ \Delta h_k/4, & r_k < 0.25 \\ \Delta h_k, & 0.25 \le r_k \le 0.75 \end{cases}$$

$$\text{s.t.} \begin{cases} \Delta h_{k+1} = \Delta h_{\min}, & \Delta h_{k+1} < \min bc \\ \Delta h_{k+1} = \min(\max bc, \max bc2), & \Delta h_{k+1} > \min(\max bc, \max bc2) \end{cases} \quad (4)$$

For a continuous multidimensional function, when the gradient value corresponding to a certain point is 0, it indicates that the function does not change with the change of the independent variables in any direction of the point. If the function near this point is a concave function, it indicates that the function value corresponding to this point is the minimum value of the function, which corresponds to the trust region parameter guidance algorithm by determining whether the function value $f(X_{k+1})$ calculated by the $(k+1)^{\text{th}}$ iteration is smaller than the function value calculated $f(X_k)$ by the k-th iteration. If it is, it indicates that the function near the point is a concave function; otherwise, it is a convex function.

When all the element values in the expression of the approximate gradient g_k obtained by the k–1 iteration are equal to 0 and the function value calculated by the $(k+1)^{\text{th}}$ iteration is greater than the function value calculated by the k-th iteration, the iterative calculation is finished, and the minimum value is $f(X_k)$. This condition for ending the iterative calculation is defined as Condition a.

In the optimization process, limited by the complexity and calculation accuracy of the objective function, the optimal function value with zero gradient may never be found. Therefore, the function value of each iteration calculation is stored in sequence according to the number of iterations, which is recorded as F_{zxjh}, and the minimum function value $\min f$ appearing in the previous iterations is updated. When the k-th calculation is performed, if the minimum function value $\min f$ and the parameter group X appear more than three times in the function value set and the parameter group recorded in the previous iterations, the iterative calculation is skipped. The minimum value is $f(X_{k+1})$, and the conditions for ending the iterative determination are defined as Condition b. When the number of iterations is greater than 2, it is determined whether Condition a and Condition b are satisfied after the completion of the current calculation. As long as one of the two conditions for ending the iterative determination is satisfied, the iterative calculation ends.

2.1 Trust region parameter-guided optimization algorithm flow chart

The specific process of the algorithm is shown in Figure 1. Compared with the process of the parameter-guided optimization algorithm, this method needs to constrain the step size while changing the step size. In addition, the determination of the end of the iterative calculation also becomes two.

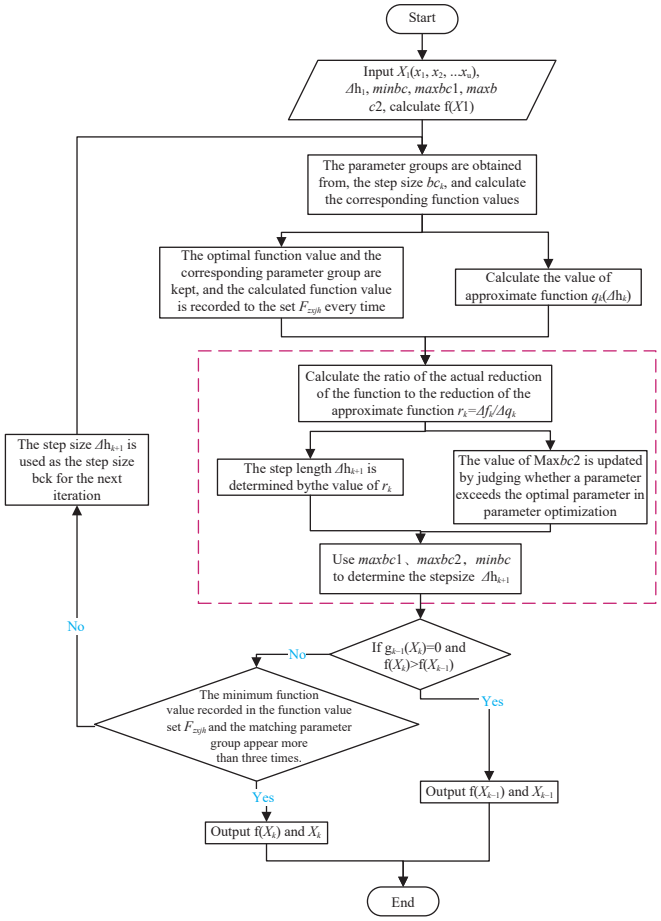

Figure 1 Trust region parameter-guided optimization algorithm flow chart

3 Multi-target trust region parameter-guided optimization algorithm

3.1 Mathematical model of the multi-target trust region parameter-guided optimization algorithm

Compared with the trust region parameter-guided optimization algorithm, in addition to initializing each parameter, a homogeneous weight vector must be generated. Since each weight of the multi-objective trust region parameter guidance method corresponds to an optimal solution and the optimization trajectory of each subproblem is guided by the weight vector, the following equation is obtained:

$$\lambda_1 + \lambda_2 + \ldots + \lambda_m = 1 \quad (5)$$

$$\lambda_i \in \left\{ \frac{0}{H}, \frac{1}{H}, \ldots, \frac{H}{H} \right\}, \ i = 1, 2, \ldots, m \quad (6)$$

The weight vectors of ownership are all valued from $\{0/H, 1/H, \ldots, H/H\}$. Only by defining a positive integer H can a set of weight vectors with a total number $N = C_{H+m-1}^{m-1}$ be obtained. In the equation, m is the number of objective functions, which is equal to the number of weight values under each weight vector. Each weight vector corresponds to a single objective subproblem, that is, to ensure that the weight vector direction can obtain the optimal function group value and the corresponding parameter group.

In the k-th iteration, the parameter groups under each weight

vector are given a parameter group with the current step size $bc(k,n)$ increasing or decreasing by a small amount,

The parameter groups under each weight vector obtain a parameter group based on increasing or decreasing step $bc(k,n)$. A total of $2u$ parameter groups are obtained, and the corresponding function group value is calculated.

In the 1st iteration (k=1), the parameter group under the ownership weight vector is obtained according to the initial parameter group $X^1(x_1,x_2,\ldots,x_u)$ of the input, and the function group values under each weight vector are the same.

Since the respective subproblems are relatively independent, multiple repeated calculations may occur during the calculation process. To avoid the above situation, a temporary dataset library with a total amount of $8u$ is established, which contains the values of each parameter group and the corresponding function group. After obtaining the parameter group X_{ni}^k to be calculated on each iteration calculation and each weight vector, the temporary database is searched. If the parameter group X_{ni}^k is not in the temporary database, the objective function group is calculated, and the function group value and the parameter group are replaced by the old data in the temporary database. In contrast, the calculation is replaced by a search to reduce the number of calculations and shorten the calculation time.

Under the subproblems corresponding to each weight vector, the obtained parameter groups must be compared with the optimal parameter group calculated in the previous iteration. There are several comparison strategies:

1) Weighted sum method: the weight vector and the old and new calculation function group value corresponding multiplication and summation. The parameter group corresponding to the smaller number is taken as the better parameter group. There are the following:

$$\min g(X \mid \lambda) = \lambda_1 f_1(X) + \lambda_2 f_2(X) + \cdots + \lambda_m f_m(X) \tag{7}$$

This method is similar to the method of giving a multi-objective function a weight into a single-objective problem to obtain a set of solutions, which is to aggregate different objective functions to solve the problem. However, in the trust region parameter-guided optimization algorithm, the parameter group values with N weight vectors can be obtained. This method is relatively simple, but it cannot reflect the solution well when the Pareto solution set is a nonconvex function.

2) The Chebyshev method: As reference point Z is continuously updated during the iterative calculation, the position relationship with reference point Z is used to select a better parameter group. There are the following:

$$\min g(X|\lambda, z^*) = \max_{1\le i\le m}\{|\lambda_i(f_i(X) - z_i^*)|\} \tag{8}$$

The number of z_i^* is the same as the number of objective functions, and all z_i^* constitute the reference point Z. The reference point is unified under each subproblem and is updated only when the function value of each function is obtained to the minimum.

Different from the selection of Z in the MOEAD method, there are two modes. One can use the trust region parameter guidance method described in Section 1.2 to calculate the minimum value of each objective function, that is, $[\min f_1, \min f_2, \ldots, \min f_m]$; this vector is used as a reference point. The other Z is that each objective function obtains the minimum value in the previous iteration and then subtracts a step size ckb. The reference point step size is the maximum value of the reduction of each objective function obtained in the last iteration under each subproblem. In the iterative calculation process, it may occur that the parameter group is not updated when the two calculations are separated. At this time, the step size follows the value of the step size used in the previous iterative calculation, as shown in Equation (9). This applies to situations where the minimum value of the objective function value is unknown or the approximate distribution of the Pareto solution set and the distance from the initial value target are uncertain.

$$\begin{cases} cbk_i = \max(|f_i(X_1^k) - f_i(X_1^{k-1})|, |f_i(X_2^k) - f_i(X_2^{k-1})|, \ldots, \\ \qquad |f_i(X_N^k) - f_i(X_N^{k-1})|), i = 1,2,\ldots,m \\ Z = [\min F_{1zxjh} - ckb_1, \min F_{2zxjh} - ckb_2, \ldots, \min F_{mzxjh} - ckb_m] \end{cases} \tag{9}$$

Through the above two methods, the corresponding parameter group X_n^{k+1} and the corresponding function group value $[f_1(X_n^{k+1}), f_2(X_n^{k+1}), \ldots, f_m(X_n^{k+1})]$ under each weight vector are updated. After each iterative calculation, the result is transformed into a matrix and stored. It can be imported externally.

Combined with the idea of the trust region parameter-guided optimization algorithm in Section 1.3, the approximate gradient $g_i(X_k)$ of each objective function at this point can be calculated by Equation (1). When $2u$ parameter groups X_{ni}^k are obtained based on the parameters in each subproblem, the approximate function q_{ik} of each objective function is calculated by Equation (2). After determining the better parameter set X_n^{k+1} after each iteration by comparing the strategies, the ratio ri_n^k of the actual reduction of each objective function and the reduction of the approximate function can be obtained from Equation (3). The minimum value of the ratio of the m objective functions is defined as the approximation degree of the approximate function and the original function of the subproblem, namely, $r_n^k = \min(r1_n^k, r2_n^k, \ldots, rm_n^k)$. The meaning is to determine the step size of the next iteration by the objective function with the worst approximation.

The values of the parameter groups X_n^k of a subproblem during the two consecutive iterations will not change. This means that the steps need to be shortened, and the fineness of the calculation is needed. Therefore, the maximum step length of the next iteration is 0.75 times that of the step size.

The method for changing the step size and updating $\max bc2$ by determining whether a parameter exceeds the optimal parameter in parameter optimization is the same as the trusted domain parameter guidance method.

After calculating all the subproblems generated by the weight venue in turn, the next iteration calculation is started. When all X_n^k and the corresponding functional group values do not change after three consecutive iteration calculations, this means that it can no longer find better parameter groups to replace the current parameter groups and jump out of the iterative calculation. In addition, a maximum iterative computing step is set, and the calculation ends after reaching the maximum iterative step.

3.2 Multi-target trust region parameter-guided optimization algorithm flow chart

According to the above-mentioned multi-target trust region parameter-guided optimization algorithm, a program and a flow chart of the algorithm that uses the Chebyshev method is written, as shown in Figure 2. Among them, the dotted frame steps are for a long time for one operation, and part of the repeated computing part will replace the search parameter array and the corresponding functional value instead of a complete calculation. This step is not necessary. The dotted line of the frame changes the step size and updates $\max bc2$ by determining whether a parameter exceeds the

optimal parameter in parameter optimization, which is consistent with the dotted line area frame in Figure 1. The green frame is calculating the functional group value of the parameter groups of each subproblem under each iteration. When the iterative jumping conditions are finally reached, the output of this step is the calculation result.

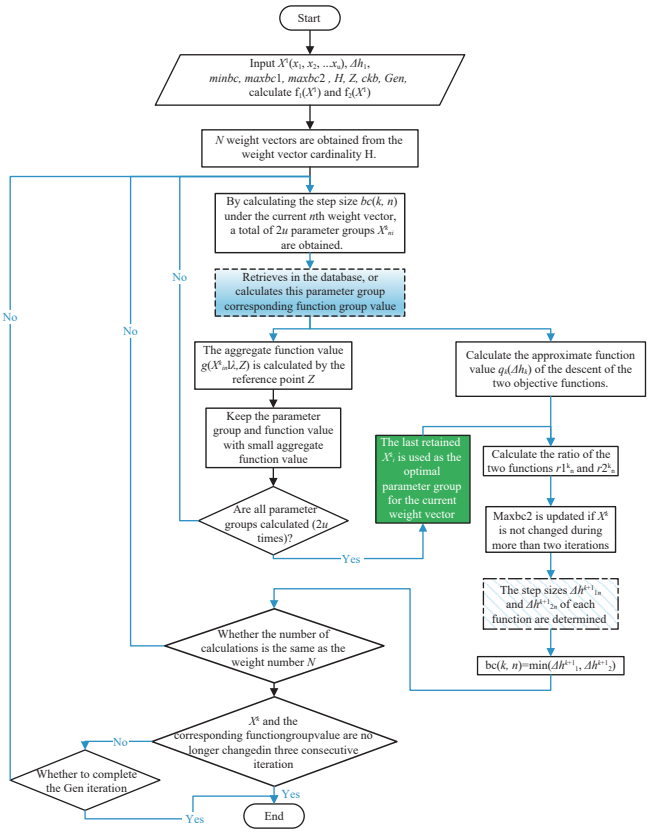

Figure 2 Multi-target trust region parameter-guided optimization algorithm

3.3 Results and analysis of test functions calculated by the multi-objective calculation method

To better test the robustness and accuracy of the algorithm, the test function of the following table is constructed. D represents the feature dimension, $f_{\min}$ represents the theoretical global optimal value of the function theory, and x_i^* represents the value of the parameter group when the minimum value of the function is taken. Since this paper mainly improves the parameter-guided algorithm, the selected functions are bowl-shaped functions with only one extreme value.

Table 1 Test function

Test function	D	$f_{\min}$	x_i^*
$F1=\sum_{i=1}^{D}(x_i-1)^2-\sum_{i=2}^{D}x_ix_{i-1}$	8	$-D(D+4)\cdot(D-1)/6$	$x_i^*=i(D+1-i),\ i=1,2,\ldots,D$
$F2=\frac{1}{2}\sum_{i=1}^{d}\left(x_i^4-16x_i^2+5x_i\right)$	8	$-39.165\ 99D$	$x_i^*=(-2.903\ 534,\ldots,-2.903\ 534)$
$F3=\sum_{i=1}^{d}\lvert x_i\rvert+\prod_{i=1}^{d}\lvert x_i\rvert$	8	0	$x_i^*=(0,\ldots,0)$

The MOEAD algorithm of the Chebyshev method is used to calculate the function groups of 8-dimensional test functions $F1$ and $F2$, $F2$ and $F3$, and $F1$ and $F3$. The boundary of each parameter is set to [–20,20], H = 14, the population dimension is 15×8, and the iterative calculation is 2000 times. Each test function group can obtain 15 sets of parameter group values and corresponding function group values. When the multi-objective trust region parameter guidance method is used to calculate each objective function group, the initial value of each parameter is set to –10, H = 14.

The concept of a congestion degree is used to determine whether the multi-objective calculation results obtained are excellent or not. The calculation method of the congestion degree is as follows:

1) The function group values obtained in the calculation results are arranged from small to large with a certain target. 2) The crowding distance of the two poles of the maximum target value and the minimum target value is defined as infinity. 3) The distance between the nearest neighbors of each individual is calculated and the maximum target value and the minimum target value are used to normalize it. 4) Traversing each target, the crowding distance is added to obtain the crowding degree. The crowding distance is shown in Equations (10) and (11).

$$dist_i[n]=\frac{f_m(X_{n+1})-f_m(X_{n-1})}{f_m^{\max}-f_m^{\min}} \tag{10}$$

$$dist=\sum_{i=1}^{m}dist_i[n] \tag{11}$$

In addition, the sum of the objective minimum values is calculated, and the minimum values of each objective function are added, as shown in Equation (12). This value can indicate the goodness of the minimum value that can be found for each objective function in the objective function group.

$$fzc=\sum_{i=1}^{m}f_m^{\min} \tag{12}$$

In the solution of the double objective problem, calculating the average crowding distance can measure the average level of uniformity of the calculation results. The maximum crowding distance can measure the isolation degree of the parameter group deviating from other solutions, and the crowding degree variance can measure the dispersion degree of the crowding degree of each target point. The smaller the two values are, the better the algorithm is. The objective minimum sum, maximum crowding distance, average crowding distance, and crowding distance variance of each combination obtained by the MOEAD algorithm are listed in Table 2.

Table 2 The indicator value obtained by each test function group calculated by two algorithms

Item	F1 and F2		F2 and F3		F1 and F3	
	MOEAD	The designed algorithm	MOEAD	The designed algorithm	MOEAD	The designed algorithm
Objective minimum sum	–424.9506	–425.3284	–313.1773	–313.3189	–87.8528	–111.9895
Maximum crowding distance	1.3894	1.3879	1.0761	1.0702	1.0068	1.7117
Average crowding distance	0.2008	0.2026	0.1894	0.1892	0.2104	0.1746
Crowding distance variance	0.1316	0.1431	0.1094	0.1064	0.0616	0.2152

Although the MOEAD method is a modern optimization

algorithm for solving multi-objective problems, the multi-target trust region parameter-guided optimization algorithm is a deterministic algorithm with a given initial value. The principle and scope of application of the two methods are different. Therefore, only the comparison of the results of the algorithm is given, and the calculation amount and calculation speed are not analyzed. The calculation results of the two-objective function group and the result index values of the two algorithms are compared.

It can be seen that there is not much of a difference between the results obtained by the $F1$ and $F2$, $F2$ and $F3$ function groups. By comparing the variance of crowding distance and the maximum crowding distance, it can be seen that the uniformity of the results obtained by the multi-target trust region parameter-guided optimization algorithm in $F1$ and $F2$ is slightly inferior to the MOEAD method, while $F2$ and $F3$ are the opposite. In the $F1$ and $F3$ objective function groups, the uniformity obtained by the multi-target trust region parameter-guided optimization algorithm is much weaker than that obtained by the MOEAD method. However, in the item of the objective minimum sum, the corresponding value of the MOEAD method is much larger than the corresponding value of the multi-target trust region parameter-guided optimization algorithm, indicating that the diversity of the results obtained by the MOEAD method is weaker than the method designed in this paper.

The next section takes the optimization design of the film-covered sweet potato transplanting mechanism as an example to illustrate the practical application of the designed algorithm.

4 The optimized design of the film-covered sweet potato transplanting mechanism

4.1 Problem description and initial parameters

Transplanting sweet potato seedlings after cover film on the field is helpful to increase the yield of sweet potatoes, and the bottom transplanting trajectory should be adopted. The transplanting trajectory also has the requirements of an adaptive horizontal transplantation distance and small film damage. The optimization design of a film-covered sweet potato transplanting mechanism that meets the transplanting requirements is a complex multi-target optimization problem.

The double planetary frame mechanism has the advantages of good transmission, small impact, and adjustable position at the working section. Therefore, this type of mechanism is used to design the film-covered sweet potato transplanting mechanism. A schematic diagram of the mechanism is shown in Figure 3. The second planet carrier is driven by two pairs of noncircular gears: the sun gear and first intermediate gear, and the third intermediate gear and planetary gear. The transplanting arm is driven by the second intermediate gear, first planetary gear, first spur gear, second spur gear, and third spur gear. The pulling line cam drives the pulling line to drive the seedling claw to realize the clamping and releasing action of the seedling. The degree of freedom of the whole machine is 1.

Taking the rotation angle of the first planet carrier as the timing sequence, the moving direction of the mechanism relative to the ground is set to the left. After transforming the dynamic pose into a static pose, the closed-loop vector method[28] is used to calculate a set of initial solutions of the mechanism that can be made into a noncircular gear set. The coordinates of the first planet carrier rotating with the ground are set as the origin of the coordinates, and the other mechanism parameters are listed in Table 3.

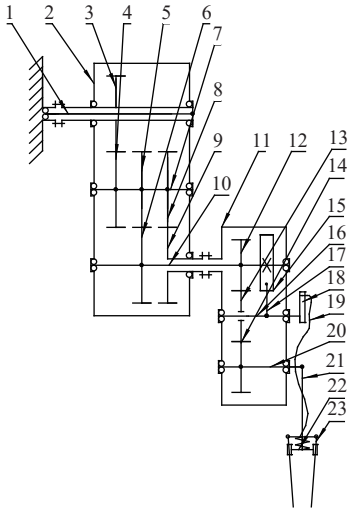

1. Sun wheel shaft 2. First planet carrier 3. Sun wheel 4. First intermediate wheel 5. Third intermediate wheel 6. Second planet wheel 7. Intermediate wheel shaft 8. Second intermediate wheel 9. First planet wheel 10. Planet wheel shaft 11. Second planet carrier 12. First spur gear 13. Second spur gear 14. Third spur gear 15. Drawing cam 16. First spur gear shaft 17. Swing rod of cam 18. Pulling swing rod 19. Pulling line 20. Second gear shaft 21. Transplanting arm 22. Clamping seat 23. Seedling clamping claw

Figure 3 Diagram of sweet potato transplanting mechanism

Table 3 Predesigned parameters of film-covered sweet potato transplanting mechanism

Item	Initial mounting angle of first planet carrier/(°)	Initial mounting angle of second planet carrier/(°)	Initial mounting angle of transplanting arm/(°)	Length of first planet carrier/mm	Length of second planet carrier/mm	Length of transplanting arm/mm	Angle of transplanting arm marking to seedling claw/(°)
Value	105.1	135.8	223.9	113.29	89.42	236.45	47

The relative rotation angle of each planet carrier is calculated when the group of rods passes through each set of postures, and cubic B-spline fitting is used to obtain the static trajectory and dynamic trajectory of the mechanism, as shown in Figure 4. Then, the pitch curves of each noncircular gear group are obtained by using the transmission ratio distribution of the noncircular gear group.

Trajectories A-B-C-D-E-F of the predesigned sweet potato transplanting mechanism are analyzed. The position P_{j1} of the seedling claw at A is the starting position of the mechanism operation. The clamping claw clamps the sweet potato seedlings from the supporting seedling feeding mechanism at point A, and the A-B section is the seedling transport section. B-C-D is the buried section, point B is the point that just entered soil, and point D is the planting point. The planting spacing of the potato seedlings was 200 mm. The bottom planting method requires that the root of potato seedlings is approximately 50 mm from the soil surface, and the horizontal transplantation distance (the horizontal distance from point D to point E) is close to 125 mm.

Because the soil surface will be covered with film before planting sweet potato seedlings, the hole formed by the film during the planting process of the sweet potato transplanting mechanism should be as small as possible. That is, when the seedling claw moves on buried Section B-C-D, the horizontal distance of the

posture of the seedling claw sweeping over the soil surface should be small. In the continuous movement of the seedling claw on the buried section, the author selects several postures of the seedling claw in Figure 4b. The posture of the seedling claw under different timings will damage the film.

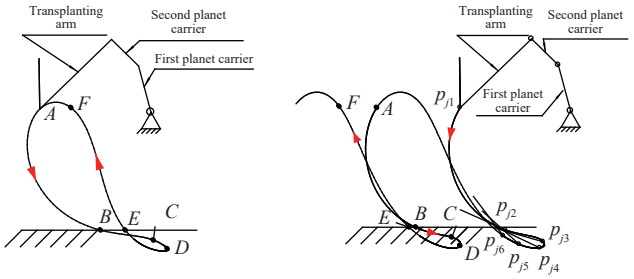

a. Static trajectory of predesigned mechanism b. Dynamic trajectory of predesigned mechanism

Figure 4 Transplanting trajectory of predesigned film-covered sweet potato transplanting mechanism

The optimal control points and the corresponding rotation angles of the first planet carrier are selected on the buried trajectory section, as shown in Table 4. By optimizing the control points and the corresponding planetary frame rotation angle of a total of 30 data points, the trajectory of the buried section of the sweet potato transplanting mechanism forms the hole during the transplanting process as small as possible under the requirement of the horizontal transplantation distance.

Table 4 Optimal control points

Number	x_{nyh}/mm	y_{nyh}/mm	Rotation angles of first planet carrier $Jc1_{nyh}$/(°)
1	–170.29	–277.86	220.47
2	–120.44	–293.71	240.05
3	–80.79	–302.80	259.89
4	–63.58	–317.02	280.98
5	–89.95	–326.98	303.52
6	–104.77	–324.31	308.08
7	–123.44	–318.28	312.84
8	–147.10	–306.88	318.25
9	–167.37	–293.59	322.84
10	–183.38	–280.52	326.65

4.2 Establish the mathematical model of the optimization mechanism

The initial parameter group G^1 is obtained by connecting the abscissa, ordinate, and rotation angle of the first planet carrier of each optimal control point in Table 4. It is denoted as the abscissa, ordinate, and the rotation angle of the first planet carrier of a control point based on the change of u–th, $(u=1,2,\ldots,10)$ optimal control points after the s-th iteration. When changing a control point at the s-th iteration, according to the rod length of each rack in Table 3 and the rotation angle of the first planet carrier, the two special-shaped positions of the mechanisms can be obtained by the rod length identity equation, as shown in Figure 5. The three-dimensional vectors $\overrightarrow{A_{ccs}A_{dcs}}=(x_{csAdr}-x_{csAcr},x_{csAdr}-y_{csAcr},0)$ and $\overrightarrow{A_{ccs}A_G}=(G_r^s-x_{csAcr},G_{r+10}^s-y_{csAcr},0)$ are set, and the z-axis component value of $\overrightarrow{A_{ccs}A_{dcs}}\times\overrightarrow{A_{ccs}A_G}$ is calculated. If the value is greater than 0, the corresponding mechanism configuration is a reasonable configuration.

Then, the rotation angle of the first planet carrier $Jccs1'$, the rotation angle of the second planet carrier $Jccs2'$, and the rotation angle of the marking line of the transplanting arm $Jccs3'$ are calculated by combining the attitude angles of each planet carrier and the picking arm of the picking claw at the initial position P_{j1}. More rotation angles of the first planet carrier $PHIcs1$, the rotation angles of the second planet carrier relative to the first planet carrier $PHIcs2$, and the rotation angles of the transplanting arm relative to the second planet carrier $PHIcs3$ are obtained by cubic B-spline interpolation fitting. Similar to the previous section, a total of six noncircular gear pitch curves are obtained according to the transmission ratio distribution of the noncircular gear group while obtaining the static trajectory point coordinates and the dynamic trajectory point coordinates of the mechanism corresponding to the parameter group.

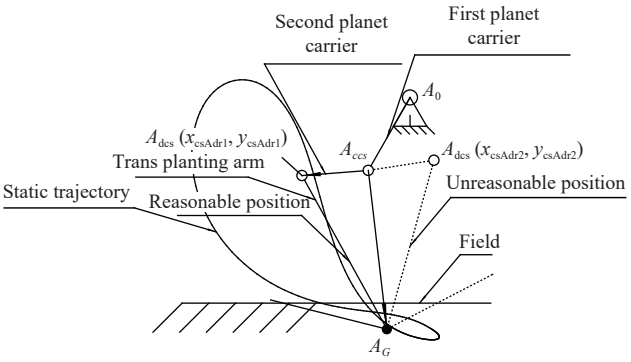

Figure 5 Two special-shaped positions of the mechanisms

Restriction conditions: The pitch curves of six noncircular gears are substituted into the noncircular gear profile generation program mentioned in this paper[29]. Whether a reasonable tooth profile can be generated is determined. If not, the parameter group is invalid.

Optimization goal 1: Meet the requirements of the horizontal transplantation distance of sweet potato transplanting.

As shown in Figure 6, the smallest ordinate value $\min y_{cspd}$ is found in the coordinates of the dynamic trajectory point (x_{cspd},y_{cspd}), all the points on the transplanting trajectory are recorded where the ordinate is less than $\min y_{cspd}+50$ as the dynamic trajectory point under field (x_{cspdx},y_{cspdx}), and the smallest value of the abscissa $\min x_{cspdb}$ is recorded in these points as the transplanting point of the sweet potato seedlings. The point with the maximum value of the abscissa $\max x_{cspdb}$ is recorded as the deepest point of the transplanting of the potato seedlings. According to the transplanting requirements of sweet potato seedlings, the distance between the deepest point of transplanting and the point that just entered soil in the horizontal direction is 125±3.5 mm.

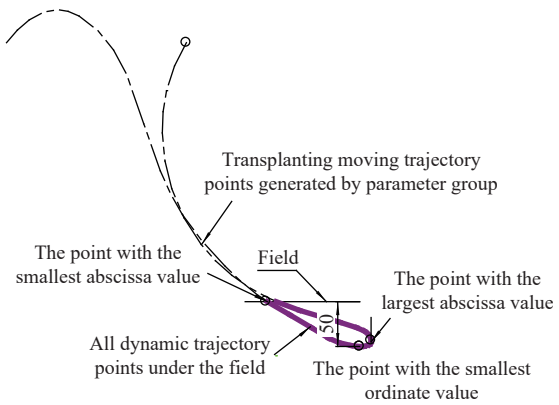

Figure 6 Schematic diagram of key points on the trajectory

The bell-shaped membership function is used to express the optimization goal of the horizontal distance between the deepest point of transplanting and the point that just entered soil in the horizontal direction. The expression of the membership function is as follows: According to the requirements of sweet potato seedling transplanting, the membership function value and the following value are defined as unsuitable horizontal transplanting values, and $c = 125$, $a = 7$, $x = 110$, $b = 3.0146$ are calculated. Considering that the closer the membership function is to 1, the better the degree of conformity is, the objective function is:

$$f_1 = 1 - \frac{1}{1 + \left| \frac{x - 125}{7} \right|^{6.0293}} \tag{13}$$

Optimization goal 2: The straight line equation of the seedlings is calculated under each trajectory point under the soil surface, that is, $y_{cs} = \tan(Jc3_1 - PHIcs3 + bsjjp) \cdot (x - x_{cspdx}) + y_{cspdx}$. Set $y_{cs} = \min y_{cspd} + 50$. The abscissa x value of the intersection point between the seedling claw and the soil surface at each dynamic trajectory point under field conditions is obtained. The maximum value of x minus the minimum value of x is the hole size f_2 formed by the machine, as shown in Equation (14):

$$f_2 = \max y_{cs}^{-1} - \min y_{cs}^{-1} \tag{14}$$

Combining two optimization objectives and one constraint, the optimization objective can be described as:

$$\begin{cases} \min F(G^s) = [f_1(G^s), f_2(G^s)] \\ \text{s.t. Each gear pitch curve can be made into non-circular gears} \end{cases} \tag{15}$$

The optimization problem has an initial parameter set. If the modern multi-objective optimization algorithm is used to solve the problem, it is difficult to limit the range of each parameter. However, the optimization problem includes 01 programming (integer programming with logical variables of 0 or 1), and the parameters in the parameter group interact with each other. The random combination will cause the noncircular gear set of the mechanism to be unable to be made, and the parameter set obtained by multiple iterations may be invalid, which is not conducive for the optimization algorithm to generate offspring based on the excellent parent. In this case, it is not easy for the multi-objective optimization algorithm to obtain the answer. If the traditional deterministic algorithm is used, the Pareto solution of the multi-objective problem cannot be obtained; additionally, since the gradient of the equation cannot be solved, the problem cannot be solved. The next section proves its practicability through the calculation algorithm designed in this paper.

4.3 Calculation results and simulation verification

Using Equations (13) and (14), the hole size of the sweet potato transplanting mechanism corresponding to the initial parameter group is 20.64 mm, and the horizontal transplantation distance is 123.19 mm. Considering the extreme case, when the optimal control points converge at point B, the hole formed by the transplanting trajectory to the soil film can be 0, and the minimum value of the optimization function f_2 can be 0. The transplanting transverse distance of the predesigned film-covered sweet potato transplanting mechanism itself conforms to the most appropriate transplanting transverse depth, and the minimum value of the optimization function can also be 0. The designed multi-objective trust region parameter guidance algorithm is used to solve the problem. This study set the reference point as [0,0], the initial step size is 0.5, the minimum step size $\min bc = 0.125$, and the maximum step size $\mathrm{Max}bc1 = 2$. H = 7. The calculation is completed after 307 iterations.

The obtained eight parameter groups were recalculated to obtain the transverse transplanting depth corresponding to each group of parameters, which are listed in Table 5. Each set of solutions has a total of 30 parameters about the position of 10 control points and the angle information of the first planet carrier. The data are too large and are not listed in this article.

Table 5 Optimization results of film-covered sweet potato transplanting mechanism

Number	Value of f_1	Horizontal transplantation distance/mm	Hole size/mm
1	0.995	108.399	2.986
2	0.989	110.195	3.467
3	0.192	119.486	8.429
4	0.126	119.922	10.314
5	0.089	120.244	10.958
6	0.011	121.673	11.745
7	0.005	122.086	12.085
8	0	124.972	17.639

Although the calculation results are not uniform, the results of the first and second groups and the sixth and seventh groups are similar, but the results of each group are greatly improved compared with the calculation results of the predesigned mechanism. The results of the eighth group showed that the minimum hole that can be formed by the mechanism is 17.4 mm under the condition of ensuring the horizontal transplantation distance of the film-covered sweet potato transplanting mechanism. The results of the first group showed that the minimum hole formed by the mechanism was 2.99 mm without considering the horizontal transplantation distance of the mechanism. There is little difference between this value and the minimum value of the optimization function set to zero when the reference point is set. The reason for this may be that the deterministic algorithm falls into the local optimum. In the step of calculating the initial value of the film-covered sweet potato transplanting mechanism by the closed-loop vector method, if other mechanism solutions are selected as the predesign mechanism, different calculation results may be obtained.

Although the calculated noncircular gear pitch curve has a slight depression, it has been determined by the tooth profile generation program mentioned in Section 3.2. The noncircular gear pitch curves in these mechanism solutions can be made into noncircular gears. This proves that after adding multiple optimal control points, to ensure that the solution of the mechanism can meet the proposed objectives, the optimized calculation results are close to the limit. It also proves the difficulties of the design of the film-covered sweet potato transplanting mechanism that meets the shape of the transplanting trajectory and the small hole of the film under the condition of ensuring that all gears can be made into noncircular gears.

Combined with the requirements of sweet potato transplanting, after comparing the calculation results between groups, the fourth group of mechanisms was selected as the required film-covered sweet potato transplanting machine. The optimized parameters of the mechanism solutions are listed in Table 6.

The pitch curve of each noncircular gear is obtained by using the tooth profile generation program, and the modeling is completed and imported into Adams for simulation. It is consistent with the design.

Table 6 The fourth group of mechanism solutions for optimal control point optimization results

Number	x_{nyh}/mm	y_{nyh}/mm	Angle of first planet carrier $Jc1_{nyh}$/(°)
1	–169.413	–278.112	219.4674
2	–120.069	–294.709	240.0455
3	–79.4101	–302.298	260.8928
4	–62.2086	–315.268	283.6001
5	–90.4523	–326.607	301.7698
6	–109.519	–324.307	307.9513
7	–126.069	–318.782	312.5918
8	–146.722	–306.626	318.2497
9	–167.62	–293.589	322.3357
10	–180.381	–279.271	327.2717

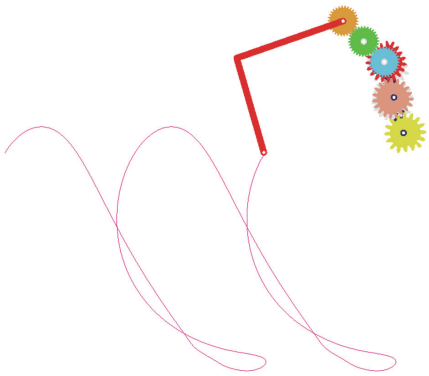

Figure 7 The fourth group of mechanism simulation results

5 Test of film-covered sweet potato transplanting mechanism

The components are assembled and the corresponding experimental platform is set up as shown in Figure 9. To test the performance of the sweet potato transplanting mechanism, two varieties, tobacco potato and watermelon red potato, are selected for experimentation. During the test, one potato seedling was sequentially placed in each slot on the triangular potato seedling conveyor belt.

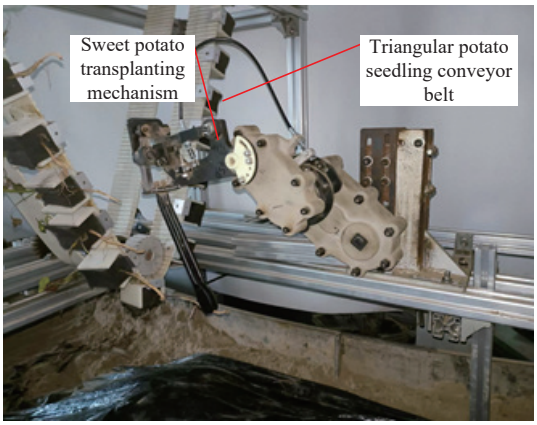

Figure 8 Experimental platform

During the experiment, the motor speed was set to 30 r/ minand the spacing between sweet potato transplants was 200 mm, so the speed of the soil trough movement was set to approximately. Two bundles of each type of sweet potato seedlings, totaling 200 plants, were used for transplanting experiments, and the success rate of seedling collection, transplanting success rate, and degree of film damage were recorded and measured.

Figure 9 shows the posture of the sweet potato transplanting mechanism during the sweet potato seedling planting stage. It can be seen that the transplanting mechanism can complete the corresponding actions well during the seedling planting stage, and the damage to the film is relatively small while completing the planting of sweet potato seedlings. This indicates that the planned design of the sweet potato seedling planting trajectory and posture in this paper is reasonable, and it also verifies the feasibility of the designed sweet potato transplanting mechanism.

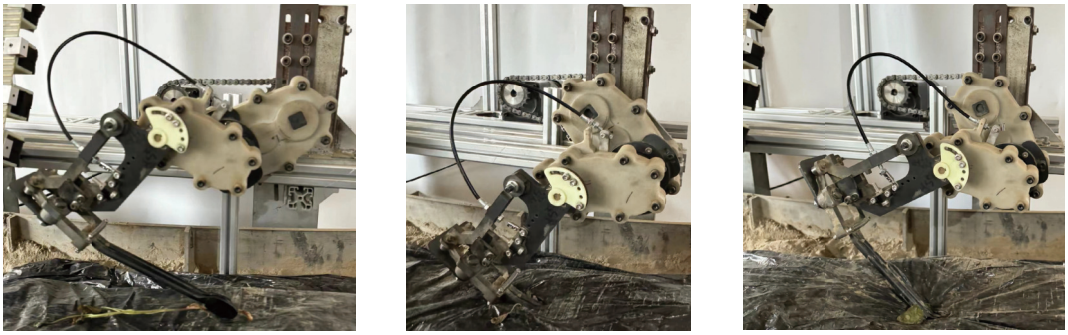

a. The beginning of planting b. At the deepest planting point c. The end of planting

Figure 9 Attitude of sweet potato transplanter at each stage of planting

The planting result is shown in Figure 10a, measuring the actual planting spacing of sweet potato transplants. The planted seedlings are marked along the surface of the plastic film, the seedlings are carefully removed, and the distance from the roots of the seedlings to the marked point is recorded. This distance is also the oblique planting depth of the sweet potato seedlings.

The slanting depth of potato seedling planting is used as the measure of transplanting effect, with depths greater than 140 mm considered successful transplantation. The planting results of two types of potato seedlings are listed in Table 7.

According to the experimental results, the transplanting success rates of two types of sweet potato seedlings by the sweet potato transplanting mechanism are both above 80%, meeting the design requirements of the automatic transplanting mechanism.

The sizes of the holes formed by the sweet potato transplanting mechanism were measured, as shown in Figure 11. The holes are generally spindle-shaped, with an average length of 50 mm. Considering that the oblique length of the end of the seedling clamping arm is approximately 45 mm, the holes created by the mulch sweet potato transplanter meet the agronomic requirements of sweet potato planting.

According to the analysis of experimental results, the main factors affecting the size of the holes created by the sweet potato transplanting mechanism are:

a. Actual planting effect diagram of seedlings

b. Measurement of oblique planting depth of seedlings

Figure 10 Actual planting results of sweet potato seedlings

Table 7 Experimental data on sweet potato seedling transplantation

Varieties	Number of seedlings	Success rate of seedling clipping	Number of successfully transplanted seedlings	Success rate of seedling transplanting
Tobacco potato	114	88.6%	94	82.56%
Watermelon red potato	93	91.4%	78	83.87%

a. Holes formed by the sweet potato transplanting mechanism

b. Measurement of hole size

Figure 11 Impact of sweet potato transplanting mechanism on film

1) The size and shape of the end of the seedling clamping arm: The larger the contact area of the end of the seedling clamping arm, the greater the tolerance of the seedling clamping, but the larger the hole formed. Improving the shape of the end of the seedling clamping arm helps puncture the film, preventing large holes caused by tearing the film.

2) Film material: Thin, flexible film is more conducive to puncturing, allowing the sweet potato transplanting mechanism to form smaller holes during planting.

3) Whether the soil surface is level and the installation position of the sweet potato transplanting mechanism relative to the height of the film surface: When designing a theoretical small hole for the double planetary gear train mechanism, it can only ensure that the surface of the film and the lowest point of planting are at the specified height to form the smallest hole. When the height of the film surface and the lowest point of planting change, the size of the hole formed will change.

6 Conclusions

This article proposed a multi-target trust region parameter-guided optimization algorithm on the basis of the trust region parameter-guided optimization algorithm. This paper used this algorithm to complete the optimization design of the film-covered sweet potato transplanting mechanism. The correctness of the results was verified, which reflected the practicability of the algorithm.

The main contributions and conclusions are as follows:

1) The mathematical model and calculation process of the trust region parameter-guided optimization algorithm were designed. Compared with the parameter guidance method, this algorithm can accelerate calculation speed while ensuring calculation accuracy.

2) Based on the trust region parameter-guided optimization algorithm, the mathematical model and calculation process of the multi-target trust region parameter-guided optimization algorithm were designed. MOEAD and this algorithm were used to calculate each test function group, which proves that the algorithm can deal well with multi-objective problems.

3) The closed-loop vector method was used to predesign the film-covered sweet potato transplanting mechanism. The hole size of the predesigned mechanism was 20.64 mm, and the horizontal transplantation distance was 123.19 mm. Then, the mechanism was optimized by using the algorithms proposed in this paper, and eight sets of results were generated for users to select. The smallest hole was 2.99 mm, and the horizontal transplantation distance was 108.40 mm. The maximum hole was 17.64 mm, and the horizontal transplantation distance of the mechanism was 124.97 mm. Considering the hole size and horizontal transplantation distance of sweet potato transplanting, a sweet potato transplanting machine with a horizontal transplantation distance of 119.92 mm and a hole size of 10.31 mm was selected. The correctness of the mechanism model was proven by Adams simulation, which proves that the multi-objective trust region parameter guidance method can effectively solve the problem.

Nomenclature

Δh: Rate of descent

q: The first-order Taylor expansion of the objective function

r: The approximation degree of the approximate function and the original function

λ: Weight vector

H: Positive integer

bc: Step

X: Parameter group

u: Number of parameter

z^*: Reference point

Jcl: Rotation angles of the first planet carrier

x_{nyh}: The horizontal coordinate of the optimal control points

y_{nyh}: The vertical coordinate of the optimal control points

G: The parameter group of mechanism

$Jccs2'$: The rotation angle of the second planet carrier

$Jccs3'$: The rotation angle of the marking line of the transplanting arm

$PHIcs1$: More rotation angles of the first planet carrier

$PHIcs2$: The rotation angles of the second planet carrier relative to the first planet carrier

$PHIcs3$: The rotation angles of the transplanting arm relative to the second planet carrier

x_{cspd}: The horizontal coordinate of the dynamic trajectory point

y_{cspd}: The vertical coordinate of the dynamic trajectory point

Acknowledgements

This work was financially supported by the Key Research Projects of China (Grant No. 2022YFD2001800), the National Natural Science Foundation of China (Grant No. 32071909), and Zhejiang Provincial Natural Science Foundation (Grant No. LD24E05007).

[References]

[1] Al-Maqtari Q A, Li B, He H J, Mahdi A A, Al-Ansi W, Saeed A. An overview of the isolation, modification, physicochemical properties, and applications of sweet potato starch. Food and Bioprocess Technology,

2023; 17: 1–32.
[2] Vithu P, Dash S K, Rayaguru K. Post-harvest processing and utilization of sweet potato: A review. Food Reviews International, 2019; 35(8): 726–62.
[3] Xu X M, Wu S Y, Chen K J, Zhang H Y, Zhou S K, Lv Z F, et al. Comprehensive evaluation of raw eating quality in 81 sweet potato (*Ipomoea batatas* (L.) Lam) varieties. Foods, 2023; 12(2): 261.
[4] Hu L L, Wang B, Wang G P, Yu Z Y, You Z Y, Hu Z C, et al. Design and experiment of type 2ZGF-2 duplex sweet potato transplanter. Transactions of the CSAE, 2016; 32(10): 8–16.
[5] Li L, Xu Y L, Pan Z G, Zhang H, Sun T F, Zhai Y M. Design and experiment of sweet potato up-film transplanting device with a boat-bottom posture. Agriculture, 2022; 12(10): 1716.
[6] Yan W, Hu M J, Li K, Wang J, Zhang W Y. Design and experiment of horizontal transplanter for sweet potato seedlings. Agriculture, 2022; 12(5): 675.
[7] Pan Z G, Li L, Chen D Q, Zha X T, Yang R B. Design and optimization of a boat-bottom-shaped transplanting device for sweet potato (*Ipomoea batatas*) with low seedling damage rate. Applied Sciences, 2022; 12(6): 2817.
[8] Wen Y S, Zhang J X, Tian J Y, Duan D S, Zhang Y, Tan Y Z, et al. Design of a traction double-row fully automatic transplanter for vegetable plug seedlings. Computers and Electronics in Agriculture, 2021; 182: 106017.
[9] Liu Z D, Lv Z Q, Zheng W X, Wang X. Trajectory control of two-degree-of-freedom sweet potato transplanting robot arm. IEEE Access, 2022; 10: 26294–26306.
[10] Liu Z D, Wang X, Zheng W X, Lv Z Q, Zhang W Z. Design of a sweet potato transplanter based on a robot arm. Applied Sciences, 2021; 11(19): 9349.
[11] Yim N H, Lee J, Kim J, Kim Y Y. Big data approach for the simultaneous determination of the topology and end-effector location of a planar linkage mechanism. Mechanism and Machine Theory, 2021; 163: 104375.
[12] Bai S. Geometric analysis of coupler-link mobility and circuits for planar four-bar linkages. Mechanism and Machine Theory, 2017; 118: 53–64.
[13] Liu W P, Han J Y, Qiu L F. On the theory and methodology of systematic analysis of positions, singular configurations, branches and circuits, and ranges of motion for planar complex linkages. Mechanism and Machine Theory, 2022; 168: 104590.
[14] Li X G, Wei S M, Liao Q Z, Zhang Y. A novel analytical method for four-bar path generation synthesis based on Fourier series. Mechanism and Machine Theory, 2020; 144: 103671.
[15] Zhang K, Yang M W, Zhang Y M, Huang Q J. Error feedback method (EFM) based dimension synthesis optimisation for four-bar linkage mechanism. Applied Soft Computing, 2023; 144: 110424.
[16] Bulatović R R, Miodragović G, Bošković M S. Modified krill herd (MKH) algorithm and its application in dimensional synthesis of a four-bar linkage. Mechanism and Machine Theory, 2016; 95: 1–21.
[17] Baskar A, Plecnik M. Synthesis of six-bar timed curve generators of stephenson-type using random monodromy loops. Journal of Mechanisms and Robotics, 2021; 13(1): 011005.
[18] Deng B. Design and experiment of transplanting mechanism of modified elliptical gear planetary gear system for sweet potato seedlings. Zhejiang Sci-Tech University, 2022.
[19] Liao H W. Design and experiment research based on solution region synthesis of planetary gear system transplanting mechanism with 3R complete rotation kinemtic pair; Zhejiang Sci-Tech University, 2021.
[20] Hu Y X. Motion synthesis and design of rice pot seedling transplanting mechanism based on constraint of output swing angle; Zhejiang Sci-Tech University, 2021.
[21] Goulet V, Li W, Cheong H, Iorio F, Quimper C-G. Four-bar linkage synthesis using non-convex optimization. Proceedings of the Principles and Practice of Constraint Programming: 22nd International Conference, CP 2016, Toulouse, France. Springer, September 5-9, 2016.
[22] Zhang Z, Zhang Y, Ning M, Zhou Z, Wu Z, Zhao J, et al. One-DOF six-bar space gripper with multiple operation modes and force adaptability. Aerospace Science and Technology, 2022; 123: 107485.
[23] Xu X, Zhou M L, Chen X G, Yang J J. Processing method of gearbox with non-circular gear train and its application in rice potted seedling transplanting mechanism. Agriculture, 2022; 12(10): 1676.
[24] Zheng Y. Optimization design and experimental of automatic transplanting mechanism for flower plug seedlings. Zhejiang Sci-Tech University, 2021.
[25] Yi J-H, Deb S, Dong J, Alavia H, Wang G-G. An improved NSGA-III algorithm with adaptive mutation operator for Big Data optimization problems. Future Generation Computer Systems, 2018; 88: 571–85.
[26] Zhang Q F, Li H. MOEA/D: A multiobjective evolutionary algorithm based on decomposition. IEEE Transactions on evolutionary computation, 2007; 11(6): 712–31.
[27] Wang W W, Dai S J, Zhao W Z, Wang C Y. Multi-objective optimization of hexahedral pyramid crash box using MOEA/D-DAE algorithm. Applied Soft Computing, 2022; 118: 108481.
[28] Subbian T, Flugrad Jr D R. Six and seven position triad synthesis using continuation methods. Journal of Machine Design, 1994; 116(2): 660–665.
[29] Ma X. Design and experiment on the flower disc transplanting mechanism of planetary gear system based on the motion analysis of 3R open chain linkage group. Zhejiang Sci-Tech University, 2020.